2003

The Effect of Processing Conditions on Varistors Prepared From Nanocrystalline ZnO

Suresh Pillai
Technological University Dublin, suresh.pillai@tudublin.ie

Declan McCormack
Technological University Dublin, Declan.mccormack@tudublin.ie

John Kelly

Ramesh Raghavendra

Recommended Citation

Pillai, S. C.* et al. (2003) The effect of processing conditions on varistors prepared from nanocrystalline ZnO *Journal of materials chemistry,* 13, 2003, 2586-2590. doi:10.1039/B306280E

JOURNAL OF Materials CHEMISTRY

The effect of processing conditions on varistors prepared from nanocrystalline ZnO†

Suresh C. Pillai,[a] John M. Kelly,*[a] Declan E. McCormack,*[b] Paul O'Brien[c] and Raghavendra Ramesh[d]

[a]*Department of Chemistry, University of Dublin, Trinity College, Dublin 2, Republic of Ireland. E-mail: jmkelly@tcd.ie; Fax: 353-1-6712826; Tel: 353-1-6081947*
[b]*School of Chemistry, Dublin Institute of Technology, Kevin Street, Dublin 8, Republic of Ireland. E-mail: declan.mccormack@dit.ie; Fax: 353-1-4024989; Tel: 353-1-4024778*
[c]*The University of Manchester, Department of Chemistry and the Materials Science Centre, Oxford Road, Manchester M13 9PL, UK*
[d]*Littelfuse Ireland Ltd., Ecco Road, Dundalk, Republic of Ireland*

Received 4th June 2003, Accepted 25th July 2003
First published as an Advance Article on the web 12th August 2003

Nanoparticles of ZnO were prepared by the reaction of ethanolic solutions of zinc acetate and oxalic acid followed by drying (80 °C) and calcination (500 °C). Subsequently varistor materials were fabricated from this nanoparticular ZnO *via* two separate routes:- a) from a "core shell" material using metal salts as additives; b) by using a conventional solid state mixing of metal oxides. Sintering (1050 °C) and subsequent electrical studies were carried out for each of these samples and they were compared with commercial varistor samples prepared under similar conditions. "Core shell" type varistor material showed considerably higher breakdown voltage (V_c = 850 ± 30 V mm^{-1}) as compared to a sample prepared by mixing with metal oxides (V_c = 683 ± 30 V mm^{-1}) or commercial varistor discs (V_c = 507 ± 30 V mm^{-1}). The high breakdown voltage obtained is attributed to the formation of more varistor-active grain boundaries per unit area.

Introduction

Varistors are electronic ceramic devices whose function is to limit voltage surges by becoming strongly conducting at a breakdown voltage (V_c).[1–4] The method of preparation, crystalline size and additive homogeneity are the critical parameters to produce a better varistor material.[5–12] Varistors with inhomogeneous microstructure can cause a large spread in current/voltage characteristics due to high local currents and this leads to the degradation of the varistor during electrical operation.[2,6,8,11] It is well documented that electrical and electronic characteristics can be altered by varying the microstructure at the grain boundaries,[2,11–15] and careful control of the microstructure is required to produce a high performance varistor. Commercial varistors are usually fabricated by solid state mixing of 0.5 to 3 μm ZnO particles with dopant oxides such as Bi_2O_3, Sb_2O_3, CoO, MnO, NiO and Cr_2O_3,[2,5–7,11] the mixed powder then being pressed and sintered at higher temperatures. The final grain size after sintering is of the order of 8–12 μm and the corresponding breakdown voltage (V_c) is around 200–300 V mm^{-1} for conventional varistors. This is equivalent to a voltage drop of 1.5–3.0 V per inter granular barrier,[2,5,8] as the breakdown voltage of the sintered body is proportional to the number of grain boundaries.

With improved chemical and physical properties over their single counterparts, "core shell" materials are potentially useful in a broad range of applications.[16–21] The shell may alter the charge, functionality and dispersibility of the colloidal core and encasing colloids in a shell of different composition may also protect the core from extraneous chemical and physical changes. By homogeneously coating each spherical particle, more varistor-active grain boundaries per unit area will be formed by dopants compared to the conventional techniques.[5] Grain growth is also expected to be much less, as each grain should be homogeneously covered with dopants (grain growth inhibitors). This may also lead to a decrease in the sintering temperature required.

In this paper we report a new procedure for the formation of nanoparticular ZnO and the preparation of varistors from it a) using materials in which the dopant oxides were deposited on the nanoparticular core; b) by simply mixing with solid metal oxides. It was hoped that these procedures would lead to varistors with higher breakdown voltage due to the large number of grain boundaries. Such materials are required for applications for device miniaturisation.

Experimental

Reagents

Zinc acetate dihydrate (Riedel-de Haen, 99.5%), bismuth(III) chloride (Aldrich, 98%), antimony(III) chloride (Aldrich, 99%), cobalt(III) chloride hexahydrate (Aldrich, 98%), manganese(II) acetate tetrahydrate (Aldrich, 99%), nickel(II) acetate tetrahydrate (Aldrich, 99%), chromium(III) nitrate nonahydrate (Aldrich, 99%) and aluminium nitrate nonahydrate (Aldrich, 99%) were used as received.

ZnO (Grillo), Bi_2O_3 (Ferro corporation), Sb_2O_3 (Cookson), CoO (Outokumpu), MnO (Campbell Chemicals), NiO (Campbell Chemicals), Cr_2O_3 (Merck), Al_2O_3 (Merck) (all reagent grade) and commercial varistor powder were supplied by Littelfuse Ltd, Dundalk.

†Electronic supplementary information (ESI) available: 1) EDX associated with HRTEM of the nano-ZnO sample before and after coating with Sb, Bi and Co; 2) HRTEM and EDX associated with HRTEM of the varistor powder calcined at 300 °C after the addition of all the dopants and 3) EDX associated with FESEM of the core shell varistor sample sintered at 1050 °C. See http://www.rsc.org/suppdata/jm/b3/b306280e/

 DOI: 10.1039/b306280e

Synthesis of nanoparticular ZnO (nano-ZnO)

In a typical experiment, zinc acetate dihydrate (10.98 g, 50 mmol) was treated with ethanol (300 ml) in a rotary evaporator at 60 °C under slightly reduced pressure. The salt was completely dissolved in 20–40 minutes. Oxalic acid dihydrate (12.6 g, 100 mmol) in ethanol (200 ml) was simultaneously prepared by stirring for 10 minutes at 50 °C. The oxalic acid solution was slowly added with stirring to the warm ethanolic solution containing Zn^{2+}. The thick white gel obtained was dried in an oven set at 80 °C for 20 hours. This xerogel was calcined by heating to 500 °C and held at this temperature for 2 hours using a ramp rate of 3 °C/min in a chamber furnace to yield nanoparticular ZnO (nano-ZnO).

Coating of dopants on nano-ZnO

Nano-ZnO (2 g, 24.5 mmol) prepared as above was dispersed in ethanol (200 ml) in a conical flask and ultrasonicated for 40 minutes. Antimony chloride (0.1471 g, 0.64 mmol) and cobalt chloride hexahydrate (0.066 g, 0.27 mmol) were dissolved in ethanol (20 ml) in a beaker. Bismuth chloride (0.081 g, 0.25 mmol) was dissolved in acetone (10 ml). Solutions of the above antimony, cobalt and bismuth chlorides were added to the ethanolic suspension of zinc oxide and stirred for 5 minutes. Ammonium carbonate (4 ml, 0.1 M) was added to the above solution and stirred for 10 minutes. (A sample was taken, dried at 80 °C and subsequently examined by HRTEM). An ethanolic solution (20 ml) of nickel acetate tetrahydrate (0.042 g, 0.17 mmol), manganese acetate tetrahydrate (0.062 g, 0.25 mmol), chromium nitrate nonahydrate (0.1032 g, 0.25 mmol) and aluminium nitrate nonahydrate (0.0017 g, 0.0046 mmol) was added to the above mixture and stirred for 20 minutes. The material thus obtained was dried in an oven at 80 °C and further calcined at 300 °C. This mixture was then plastified with 1 drop each of 10% aqueous solution of poly(vinyl alcohol) and poly(ethylene glycol) and 0.015 g of gum arabic. This was further dried in an oven (100 °C) for 5 minutes and pelletised into 7 mm (diameter) × 0.7 mm (thickness) discs before sintering at 1050 °C for 2 hours in a furnace. The average thickness of the sintered pellets was 0.65 mm.

Addition of dopants to nano-ZnO using conventional solid state mixing

Nano-ZnO was mixed with commercial oxide additives by conventional solid state mixing technique. In a typical experiment nano-ZnO (2g, 24.5 mmol) calcined at 500 °C was added to Bi_2O_3 (0.06 g, 0.13 mmol), Sb_2O_3 (0.094 g, 0.32 mmol), MnO (0.022 g, 0.25 mmol), NiO (0.012 g, 0.16 mmol), CoO (0.021 g, 0.28 mmol), Cr_2O_3 (0.0196 g, 0.13 mmol) and Al_2O_3 (0.00048 g, 0.0047 mmol) and mixed in an agate mortar for 5 minutes. This mixture was then plastified, dried, pelletised and sintered as above.

Instrumentation

Infrared spectra of samples dispersed in KBr were recorded on a Genesis II FTIR Spectrometer. Measurements were carried out in the wavenumber range 400–4000 cm^{-1}.

Differential Scanning Calorimetric (DSC) measurements were performed with a Rheometric Scientific DSC QC. A small amount of sample (less than 3 mg) was heated from room temperature to 500 °C at a constant heating rate of 10 °C/minute under nitrogen atmosphere. Thermo-Gravimetric Analysis (TGA) was carried out using a Thorn Scientific TG-750 instrument operated at a constant heat flow of 1 °C/min.

Samples for powder X-ray Diffraction (XRD) were prepared by making a thin film of the powder with acetone on a glass plate and the measurement was performed with a Siemens D 500 or Philips PW 1540 X-ray diffractometer. The particle sizes were calculated by using the Scherrer equation.[13]

$$\text{Crystalline size} = \frac{0.9\lambda}{\text{B}\cos\theta}$$

where λ = X-ray wavelength, θ = Bragg angle B = line broadening. The line broadening B is measured from the increased peak width at half the peak height and is obtained from Warren formula $B^2 = B_M{}^2 - B_S{}^2$ where B_M is the measured peak width and B_S is the corresponding width of a peak of a standard material (commercial ZnO) whose particle size is greater than 200 nm.

Transmission electron microscopy (TEM) was performed with a Hitachi 7000 TEM or Philips CM 20 HRTEM (High Resolution Transmission Electron Microscope). 400 mesh copper grids coated with Formvar were used to prepare the samples. Scanning Electron Microscopic (SEM) studies were carried out by FESEM (Hitachi S-4300), which was operated at 5.0 kV or 20 kV. Samples for analysis were mounted on aluminium stubs and coated with graphite.

The BET surface area analysis was carried out using a Micromeritics Gemini 2370 instrument operating at liquid nitrogen temperature after degassing the samples for 2 hours at 200 °C.

Density measurements of the pre-sintered and sintered samples were performed in water using an Ohaus densitometer 470007-010.

I–V characteristics from 0.1 μA to 10 mA were measured by using a Keithley Instrument (Model 2410). The breakdown voltage (V_c) was measured as the voltage at a current density of 1 mA. The nonlinear constant α was calculated by measuring the voltage V_2 and V_1 at current densities I_2 and I_1 (10 mA and 1 mA) respectively and using the relationship:

$$\alpha = \frac{\log \text{I}_2 - \log \text{I}_1}{\log \text{V}_2 - \log \text{V}_1}$$

Results and discussion

Synthesis of nano-ZnO

Reaction of an ethanolic solution of zinc acetate with an ethanolic solution of oxalic acid produced a thick semi-gel. Subsequent drying at 80 °C and calcination of this gel at 500 °C produced ZnO as identified by its powder X-ray diffraction pattern (Fig. 1).

The powder X-ray diffraction pattern shows 2θ values and relative intensities (except for the 002 plane) of the peaks coincident with JCPDS data of zincite. Broadening of the X-ray bands allowed an estimate of the average particle size as 27 ± 5 nm using the Scherrer equation.[13] This was confirmed using transmission electron microscopy (Fig. 2) which revealed that the material consisted of agglomerates of spherical particles with a diameter of 34 ± 5 nm. The BET surface area for material calcined at 500 °C was found to be 17 $m^2\ g^{-1}$.

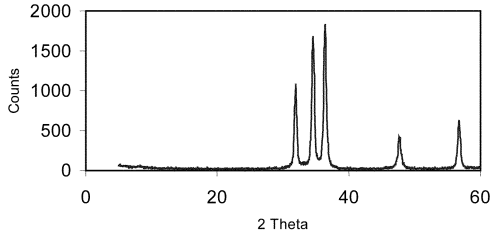

Fig. 1 X-ray powder diffraction plot of ZnO material calcined at 500 °C.

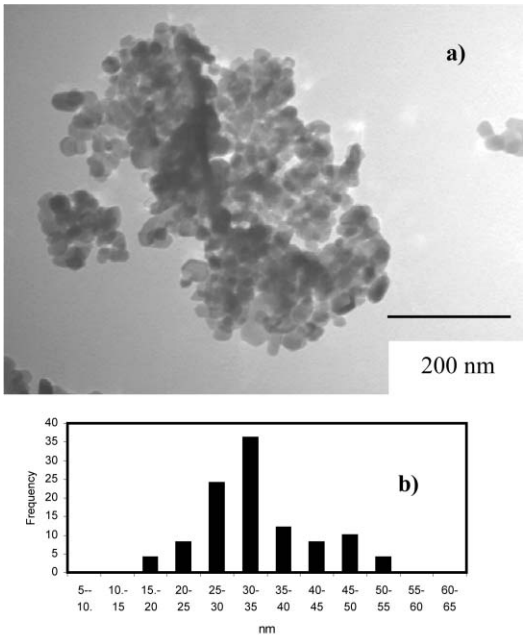

Fig. 2 a) TEM image of ZnO powder calcined at 500 °C. b) Size histogram (TEM) of the nano-ZnO.

FTIR analysis of the dried and calcined powder

The FTIR spectrum of the xerogel (80 °C) retains some typical features of an acetate salt.[14] Two principal peaks are observed at 1627 cm^{-1} and 1364 cm^{-1} corresponding to the asymmetric and symmetric stretching of the carboxyl group respectively.[14] The bands at 3398 cm^{-1} and 2900 cm^{-1} are due to OH stretching and CH (acetate) stretching respectively (Table 1).

After heating to 250 °C the sample shows evidence for the presence of carboxylate groups but the characteristic peaks for the CH_3 of acetate (2900 cm^{-1}) are absent, suggesting the loss of acetic acid. Furthermore most of the water has been lost as evidenced by the weakening of the peak around 3400 cm^{-1}. The 500 °C calcined sample is dominated by a very strong band at 450 cm^{-1} due to the Zn–O stretching. The small signal at 3411 cm^{-1} observed is probably due to the contact of the ZnO sample with air resulting in adsorption of a small amount of water vapour.[15]

Thermal analysis of the xerogel

The thermogravimetric analysis of the xerogel (80 °C) shows two stages of mass loss (Fig. 3). The first stage (80–176 °C) involves a loss of 17% of the original mass and may be attributed to the removal of water and acetic acid. In the next stage, 48.5% of the material present at 176 °C is lost by 435 °C. The residual mass (51.5%) is close to the theoretical percentage of ZnO (53.0%) found from decomposition of anhydrous zinc oxalate.

DSC showed two well-defined endotherms with peaks at 160 and 440 °C (Fig. 4). These results are fully in agreement with the IR and TGA measurements showing the loss of acetic acid/water below 200 °C and with the subsequent conversion of zinc oxalate to ZnO at 440 °C. It is possible that the reaction is similar to that reported by Shen *et al*,[22] where ZnO is formed by a solid state reaction of zinc acetate and oxalic acid and to that of Guo *et al*,[23] where ZnO is obtained from the decomposition of $ZnC_2O_4{\cdot}2H_2O$.

Table 1 FTIR analysis of the ZnO precursor gel dried at 80 °C (xerogel) and the xerogel calcined at 250 and 500 °C

Assignment	80 °C	250 °C	500 °C
ν_{asCOO-}	1627 vs	1621 s	
ν_{aCOO-}	1364 s	1364 s	
δ_{COO-}	740 s	750 w	
ν_{OH}	3398 s	3402 w	3411 vw
ν_{CH} (CH_3)	2900 vw		
$\nu_{Zn\text{-}O}$ (ZnO)			450 vs

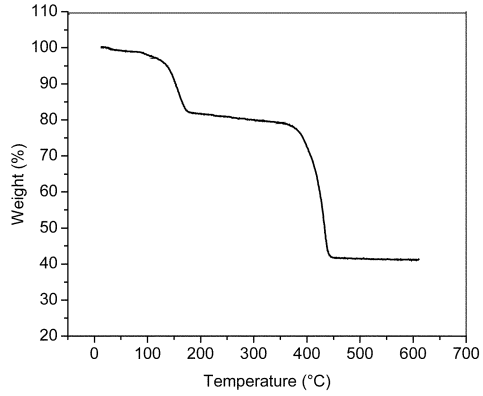

Fig. 3 TGA plot of the xerogel (80 °C).

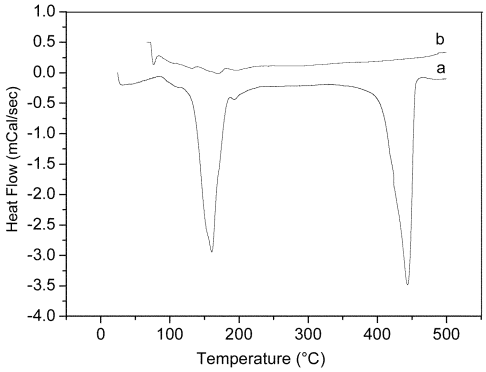

Fig. 4 DSC plot of the xerogel (80 °C) a) First scan b) Second scan.

Coating of dopants

To achieve a homogeneous coating of (Sb, Bi, and Co) oxides around the ZnO particle, solutions of chloride salts of these elements were mixed with a dispersion of nano-ZnO (as prepared above) and reacted with ammonium carbonate. This material was examined by HRTEM, which showed that the zinc oxide particles were modified by the precipitation of the Sb, Bi and Co (Fig. 5). A core of well-formed zinc oxide (with a diameter of ~25 nm) is covered by a poorly densified layer some 2 to 10 nm thick, presumably due to the carbonates of Sb,

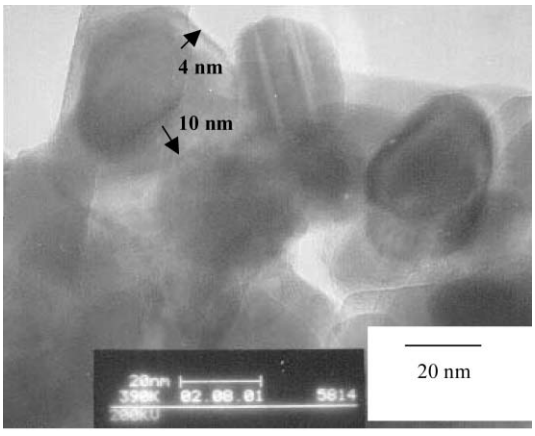

Fig. 5 HRTEM of ZnO nanoparticles coated with (Sb, Bi and Co) oxide precursors.

Table 2 Geometrical density values of the green (pre-sintered) samples

Varistor sample	Geometrical density/g cm^{-3}	Densification (%)
"Core shell" (A)	3.35	59.88
Metal oxides (B)	3.32	59.20
Commercial (C)	3.78	60.00

Bi and Co. The presence of Sb, Bi and Co were further confirmed by EDX analysis (ESI Fig. S1). The above mixture was then mixed with an ethanol solution of nickel acetate, manganese acetate, chromium nitrate, and aluminium nitrate dried at 80 °C and subsequently calcined at 300 °C for 2 hours to remove any organic residue. This material was used to make varistor discs. EDX associated with HRTEM (ESI Fig. S2) of this material showed the presence of Ni, Cr, Mn, Co and Al. HRTEM (ESI Fig. S2 a and b) studies indicate that the size of these particles were in the range of 20 to 50 nm. Core shell structure was not obvious in this case. This is probably due to the formation of dopant metal oxides from carbonates over the ZnO core while calcining at 300 °C.

Varistor properties of the doped ZnO materials

Densification studies. Two routes to varistor material were followed: A) from the mixture prepared from "core shell" material and B) by solid state mixing of nano-ZnO with metal oxide dopants. Table 2 provides the average geometrical density values of these green (pre-sintered) pellets. It may be observed that both (A) and (B) were found to be consistent with the commercial varistor samples (where the ZnO is *ca.* 0.5 μm in diameter).

These pellets were then sintered at 1050 °C and their density and electrical properties subsequently measured. These were then compared to those of a commercial varistor material (Table 3). It is clear that the varistors prepared from the novel post-treated "core shell" samples have achieved a higher densification than the others at this relatively low processing temperature. The better sintering in the former case can be explained by the homogeneous addition of dopant ions among the grains.[6]

Microstructural and electrical studies. Most metal oxide varistors contain ZnO grains as the major component with several other metal oxides as additives. ZnO without any additives is a nonstoichiometric n-type semiconductor with linear I–V behaviour. Each of the additives control one or more of the properties such as electrical characteristics, grain growth and sintering temperature.[1,2] During sintering different phases are formed and the microstructure of a ZnO varistor comprises conductive ZnO grains surrounded by electrically insulating grain boundaries. The breakdown voltage of a sintered body is proportional to the number of grain boundaries between the electrodes.[1,24] This therefore determines that the breakdown voltage depends inversely on the ZnO grain size. As the nanocrystalline material contains large grain boundary volumes, more varistor-active grain boundaries per unit volume can be produced, potentially leading to smaller dimension devices.

EDX analysis along with FESEM of the sintered "core shell"

Table 3 Densification and electrical properties of samples sintered at 1050 °C for 2 h

Varistor sample	Sintered density/g cm^{-3}	Densification (%)	Vc (± 30)/V	α (±3)
"Core shell" (A)	5.45	97.21	850	33
Metal oxides (B)	5.17	92.28	683	30
Commercial (C)	5.40	96.44	507	48

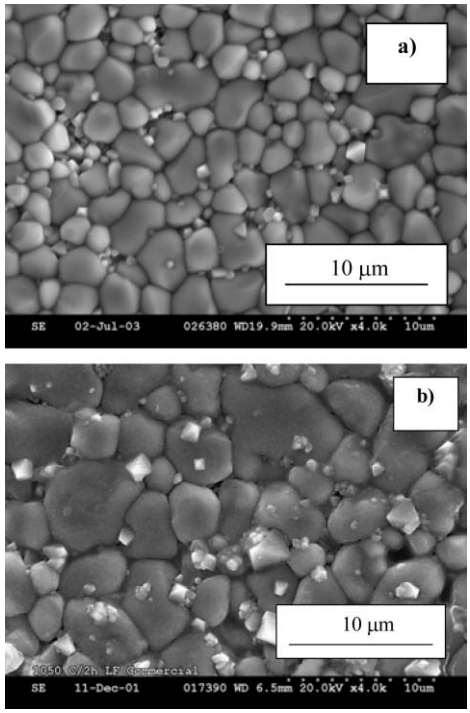

Fig. 6 FESEM images of the varistor samples sintered at 1050 °C. a) "Core-shell" samples b) Commercial samples.

(ESI Fig. S3) and commercial samples show that dopants Sb, Bi, Co, Cr, Ni and Mn are organised along the intergranular region. FESEM studies (Fig. 6) indicate a comparatively smaller average grain size (1.5 μm) for "core shell" samples compared to the commercial samples (3 μm).

The electrical properties of the sintered materials were studied. Breakdown voltages (V_c) and α values are given in Table 3. These results (Fig. 7) show a breakdown voltage V_c = 507 ± 30 V mm^{-1} for commercial samples. Considerably higher V_c (683 ± 30 V mm^{-1}) was obtained for varistors made from nano-ZnO mixed with metal oxides as additives, indicating that the smaller sized ZnO material somewhat improves the breakdown voltage. However, a much more striking effect was found with the varistors prepared from "core shell" materials, which showed much higher V_c (850 ± 30 V mm^{-1}) than that of the other two samples. This may be due to the fact that the "core shell" procedure produces a varistor powder with a greater homogeneity of the additives.

The above results point towards the formation of more grain boundaries by nano-structuring. This study has concentrated mainly on the grain size effect to achieve a high breakdown voltage, as this is the varistor property controlled by grain size. So far no effort has been made to optimise the α value, which could be facilitated by the variation of the dopant concentrations or alteration of the processing route.

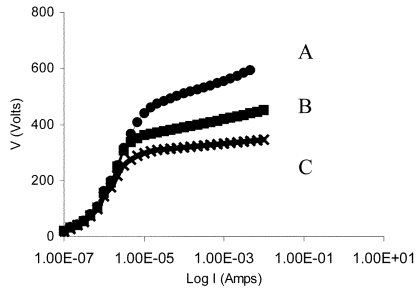

Fig. 7 I–V curve of varistor samples sintered at 1050 °C/2 hr. A = varistors prepared from "core shell" samples. B = varistors prepared from nano-ZnO and metal oxides C = commercial varistor (the average thickness of the pellets was 0.65 mm).

Conclusions

A novel method for the preparation for nano-ZnO has been successfully performed and the material characterised by XRD and TEM. Thermal analysis and FTIR results are consistent with the formation of anhydrous zinc oxalate as an intermediate. ''Core shell'' type varistor powders were prepared by coating this nano-ZnO with additive metal salts. These materials showed a superior breakdown voltage, $\sim$70% higher than that of commercial varistors and also greater than the samples prepared simply by mixing nano-ZnO and metal oxides. These improvements are those expected from the smaller grain size and additive homogeneity produced by our ''core shell'' approach. With further modification, to improve the non-linearity and sintering, this novel route should be useful for the development of higher performance miniaturised devices.

Acknowledgements

The authors gratefully acknowledge the financial support of Enterprise Ireland (ARG/HE/1998/256), Littelfuse Ireland Ltd, PRTLI (Materials) and Enterprise Ireland/British Council (BC/2001/040). We thank the Centre for Microscopy and Analysis Trinity College Dublin and the Electron Microscopy Unit Manchester Materials Science Centre for their help with TEM and HRTEM respectively, Dr M. Venkatesan, Department of Physics, Trinity College Dublin, for thermogravimetric analysis and Mr Kevin Travers, Littelfuse Ireland, for help with sample preparation.

References

1 D. R. Clarke, *J. Am. Ceram. Soc.*, 1999, **82**, 485.
2 T. K. Gupta, *J. Am. Ceram. Soc.*, 1990, **73**, 1817.
3 M. Matsuoka, *Jpn. J. Appl. Phys.*, 1971, **10**, 736.
4 L. M. Levinson and H. R. Philip, *Ceram. Bull.*, 1986, **65**, 639.
5 R. N. Viswanath, S. Ramasamy, R. Ramamoorthy, P. Jayavel and T. Nagarajan, *Nanostruct. Mater.*, 1995, **6**, 993.
6 P. Duran, F. Capel, J. Tartaj and C. Moure, *J. Am. Ceram. Soc.*, 2001, **84**, 1661.
7 G. Westin, A. Ekstrand, N. Nygren, R. Osterlund and P. Merkelbach, *J. Mater. Chem.*, 1994, **4**, 615.
8 S. Hingorani, V. Pillai, P. Kumar, M. S. Multani and D. O. Shah, *Mater. Res. Bull.*, 1993, **28**, 1303.
9 C. W. Nahm, *Solid State Commun.*, 2003, **126**, 281.
10 S. Hishita, Y. Yao and S-I. Shirasaki, *J. Am. Ceram. Soc.*, 1989, **72**, 338.
11 S. M. Haile, D. W. Johnson, Jr. G. H. Wiseman and H. K. Bowen, *J. Am. Ceram. Soc.*, 1989, **72**, 2004.
12 A. Sinha and B. P. Sharma, *Mater. Res. Bull.*, 1997, **32**, 1571.
13 A. R. West, *Solid State Chemistry and Its Applications*, John Wiley & Sons, London, 1984, p. 174.
14 E. Reverchon, G. D. Porta, D. Sannino and P. Ciambelli, *Powder Technol.*, 1999, **102**, 127.
15 A. E. Jimenez-Gonzalez, J. A. S. Urueta and R. Suarez-Parra, *J. Cryst. Growth*, 1998, **192**, 430.
16 Y. Fangli, H. Peng, Y. Chunlei, H. Shulan and L. Jinlin, *J. Mater. Chem.*, 2003, **13**, 634.
17 A. Glozman and E. Lifshitz, *Mater. Sci. Eng., C.*, 2001, **15**, 17.
18 G. Oldfield, T. Ung and P. Mulvaney, *Adv. Mater.*, 2000, **12**, 1519.
19 A. Kay and M. Gratzel, *Chem. Mater.*, 2002, **14**, 2930.
20 M. A. Malik, P. O'Brien and N. Revaprasadu, *Chem. Mater.*, 2002, **14**, 2004.
21 C. Huber, M. Treguer-Delapierre, C. Elissalde, F. Weill and M. Maglione, *J. Mater. Chem.*, 2003, **13**, 650.
22 R. J. Shen, D. Z. Jia, Y. M. Qiao and J. Y. Wang, *J. Inorg. Mater.*, 2001, **16**, 625.
23 L. Guo, Y. Ji, H. Xu, Z. Wu and P. Simon, *J. Mater. Chem.*, 2003, **13**, 754.
24 T. Asokan and R. Freer, *J. Mater. Sci.*, 1990, **25**, 2447.